Analysis of a single-atom dipole trap

Markus Weber,* Jürgen Volz, and Karen Saucke

Department für Physik, Ludwig-Maximilians-Universität München, D-80799 München, Germany

Christian Kurtsiefer

Department of Physics, National University of Singapore, Singapore, Singapore

Harald Weinfurter

Department für Physik, Ludwig-Maximilians-Universität München, D-80799 München, Germany
and Max-Planck-Institut für Quantenoptik, 85748 Garching, Germany

We describe a simple experimental technique which allows us to store a single ^{87}Rb atom in an optical dipole trap. Due to light-induced two-body collisions during the loading stage of the trap the maximum number of captured atoms is locked to one. This collisional blockade effect is confirmed by the observation of photon antibunching in the detected fluorescence light. The spectral properties of single photons emitted by the atom were studied with a narrow-band scanning cavity. We find that the atomic fluorescence spectrum is dominated by the spectral width of the exciting laser light field. In addition we observe a spectral broadening of the atomic fluorescence light due to the Doppler effect. This allows us to determine the mean kinetic energy of the trapped atom corresponding to a temperature of 105 μK. This simple single-atom trap is the key element for the generation of atom-photon entanglement required for future applications in quantum communication and a first loophole-free test of Bell's inequality.

PACS number(s): 32.80.Pj, 03.67.−a, 42.50.Vk, 42.50.Ar

I. INTRODUCTION

The coherent control of a single quantum emitter is a crucial element for the effective generation of single photons and even more for the generation of entanglement between the emitted photon and the radiating quantum system [1–5]. It is thus of fundamental importance for future applications in quantum communication and information processing, like quantum networks [6] or the quantum repeater [7]. So far, a great variety of possible experimental schemes has been worked out, based upon the control of fluorescence from different kinds of emitters, like ions [8,9], atoms [10,11], molecules [12,13], color centers [14,15] or semiconductor structures [16,17].

Cold atoms—isolated from the environment by the use of standard laser cooling and trapping techniques—are outstanding candidates for future applications in quantum networking. On the one hand, narrow-band atomic transitions can be used for the generation of single photons. On the other hand, due to the intrinsic clarity of the well defined internal level structure, atoms are also well suited for the realization of a long-lived quantum memory. In particular, a single laser cooled ^{87}Rb atom, localized in a far-off-resonance optical dipole trap (FORT) [11,18], lends itself to store quantum information in the level structure of the atomic ground state 5 $^2S_{1/2}$ for a long time with a very small relaxation rate [19]. The stored quantum information can in principle be converted to flying qubits (photons) at a wavelength of 780 nm—suitable for low-loss communication—

and therefore be transmitted between specified remote locations. And most important, the spontaneous decay of a single ^{87}Rb atom prepared in the 5 $^2P_{3/2}$, $F'=0$ hyperfine level can be used to generate entanglement between the spin state of the atom and the polarization of the emitted photon [1,5] necessary for the scalable coupling of quantum memories [20].

In this paper, we report the observation and analysis of a single ^{87}Rb atom in an optical dipole trap that operates at a detuning of 61 nm from atomic resonance. Atoms stored in this FORT have a very low photon scattering rate and therefore negligible photon recoil heating. Confinement times up to 4 s are achieved with no additional cooling. Because of the small trap volume, only a single atom can be loaded at a time [21]. To prove this property the photon statistics of the detected fluorescence light has been studied with a Hanbury-Brown-Twiss (HBT) setup. The measured second-order correlation function exhibits strong photon antibunching verifying the presence of a single atom in the trap. In addition the two-photon correlations show coherent dynamics of the population of the atomic hyperfine levels involved in the excitation process. The observed correlations cannot be explained by the simple model of a two-level atom [22]. In order to simulate the second-order correlation function of the measured fluorescence light, we numerically solve optical Bloch equations based on a four-level model. Within experimental errors we find good agreement of the theoretical predictions with the experimental data. Furthermore, we analyze the spectral properties of the emitted photons with a scanning Fabry-Perot interferometer (FPI). Due to the Doppler effect we observe a broadening of the Rayleigh scattered atomic fluorescence spectrum relative to the spectral distribution of the exciting laser light field. This broadening allows us to

---

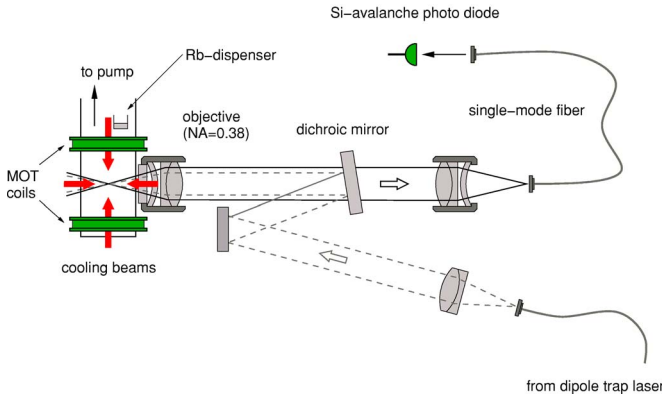*Electronic address: markus.weber@physik.uni-muenchen.de

FIG. 1. (Color online) Experimental setup of the dipole trap and fluorescence detection. The dipole trap laser is focused at the intersection of three pairs of counterpropagating laser beams for optical cooling. Fluorescence light is collected with a microscope objective, coupled into a single mode optical fiber, and detected with a Si APD.

determine the mean kinetic energy of the trapped atom corresponding to a temperature of 105 μK.

II. EXPERIMENTAL SETUP

In our experiment the FORT is generated by a Gaussian laser beam of a single mode laser diode at a wavelength of 856 nm, which is focused down with a microscope objective (located outside the vacuum chamber) to a waist of 3.5 ± 0.2 μm (see Fig. 1). For a laser power of 44 mW we calculate a trap depth of 1 mK and a photon scattering rate of 24 s^{-1} [23]. In order to load atoms into this FORT, we start with a cloud of laser cooled atoms in a magneto-optical trap (MOT) [24]. The MOT is loaded from the thermal rubidium background gas produced by a dispenser operating slightly above threshold (residual gas pressure below 10^{-10} mbar). This provides a macroscopic reservoir of cold atoms with a typical temperature on the order of 100 μK. The dipole trap overlaps with the MOT and thus by changing the magnetic field gradient of the MOT we can adjust the loading rate of atoms into the dipole trap from 0.2 s^{-1}, without quadrupole field, up to 1 atom per second at a magnetic field gradient of 1 G/cm. To assure optimal conditions for laser cooling in the dipole trap, the magnetic field is compensated below a residual value of 300 mG by three orthogonal pairs of Helmholtz coils generating a suitable bias field.

The fluorescence light scattered by atoms in the dipole trap region is collected with the focusing objective and separated from the trapping beam with a dichroic mirror. Then it is coupled into a single mode optical fiber for spatial filtering and detected with a Si avalanche photodiode (APD). In this way it is possible to suppress stray light from specular reflections of the cooling beams and fluorescence light from atoms outside the dipole trap.

To load a single atom into the FORT, we switch on the cooling and repump laser of the MOT and measure the fluorescence counting rate from the dipole trap. If a cold atom enters the trap we observe an increase of the detected fluo-
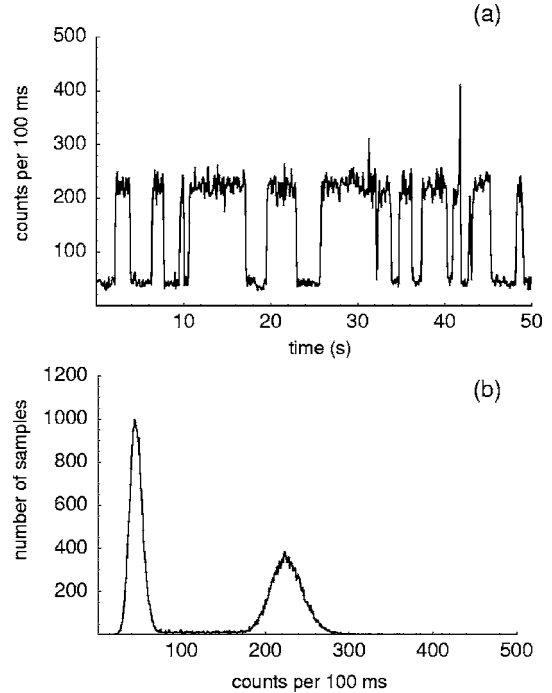

FIG. 2. Single atom detection. (a) Number of photons counted by an avalanche photodiode per 100 ms. (b) Histogram of the photon-counting data. Due to a collisional blockade effect [5,21] only counts corresponding to zero or one atom are observed.

rescence count rate. Typical photon counting rates are 500–1800 s^{-1} per atom depending on the detuning and intensity of the cooling laser. From the overlap of the detection beam (waist: 2.2 ± 0.2 μm) with the emission characteristics of the emitted atomic fluorescence we calculate an overall detection efficiency for single photons of 0.1% including transmission losses and the quantum efficiency of our Si APD.

The fluorescence rate exhibits the typical telegraph-signal structure (see Fig. 2) jumping between background intensity (450 s^{-1}) when no atom is in the trap and a defined intensity level (2250 s^{-1}) corresponding to one atom. Other fluorescence intensities have hardly been observed. This effect is caused by light-induced two-body collisions, that together with the small dipole trap volume give rise to a blockade mechanism which assures that only a single atom is trapped per time. If a second atom enters the trap, inelastic two-body collisions [25] lead to an immediate loss of both atoms [21]. We emphasize, that so far, a random telegraph signal was considered typical, when the dark phase corresponds to the same atom as the bright one does, but with the atom being shelved in a so-called dark state [26]. In contrast, here a single atom enters and leaves the trap. From the fluorescence trace in Fig. 2 we determined a $1/e$ lifetime in the presence of cooling light of 2.2 ± 0.2 s. The mean lifetime without cooling light is 4.4 ± 0.2 s. Due to the interaction with the far-off resonant dipole trap laser field, spontaneous Raman scattering leads to a change of the population occupation of an atom initially pumped to the $F=1$ hyperfine ground level. This hyperfine state changing scattering rate was determined in a measurement, similar to [19], to 0.1 s^{-1} for a trap depth of 0.75 mK.
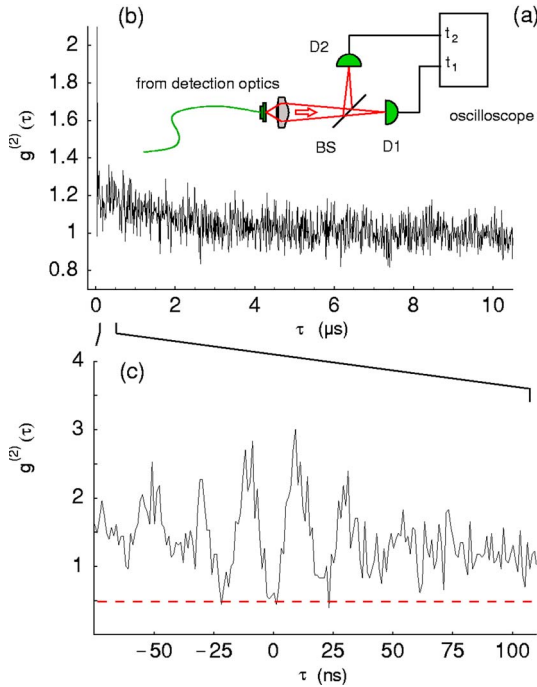
FIG. 3. (Color online) (a) Hanbury-Brown-Twiss setup for the measurement of the photon pair correlation function $g^{(2)}(\tau)$. The fluorescence light is sent through a beamsplitter (BS) onto two single photon detectors D1, D2 to record detection time differences $\tau=t_1-t_2$. (b) On long time scales, $g^{(2)}(\tau)$ shows a small bunching effect for $|\tau|\lesssim 3$ μs. (c) On short time scales, clear photon antibunching at $\tau=0$ and oscillations due to Rabi flopping are observed. The dashed line corresponds to accidental coincidences caused by the dark count rate of the detectors. Experimental parameters: I_{CL} =103 mW/cm^2, I_{RL}=12 mW/cm^2, $\Delta_{CL}/2\pi=-31$ MHz, dipole trap depth U=0.38 mK.

III. PHOTON STATISTICS

To assure that the upper fluorescence level corresponds to a single trapped atom, we analyzed the nonclassical properties of the emitted fluorescence light. For this purpose the second-order correlation function $g^{(2)}(\tau)$ was measured in a Hanbury-Brown-Twiss configuration with two detectors behind a 50:50 beamsplitter [inset (a) of Fig. 3]. The differences of detection times $\tau=t_1-t_2$ of photon pair events were recorded in a storage oscilloscope with a conditional trigger mode. To minimize background contributions, the coincidences are acquired only at times when the fluorescence exceeded a threshold of 1200 counts per s.

A normalized distribution of time differences τ is equivalent to the second-order correlation function as long as τ is much smaller than the mean time difference between two detection events [27]. For correct normalization of the measured $g^{(2)}(\tau)$ we divide the coincidences in each time bin $\Delta\tau$ by $r_1\cdot r_2\cdot\Delta\tau\cdot T$, where r_1 and r_2 are the mean count rates of the two detectors, and T is the total measurement time with an atom in the trap.

The resulting pair correlation function $g^{(2)}(\tau)$ for a trap depth U=0.38±0.04 mK, a cooling laser intensity I_{CL} ≈103 mW/cm^2, and a detuning $\Delta_{CL}/2\pi$ of −31 MHz is shown in Fig. 3. On a μs time scale the correlation function
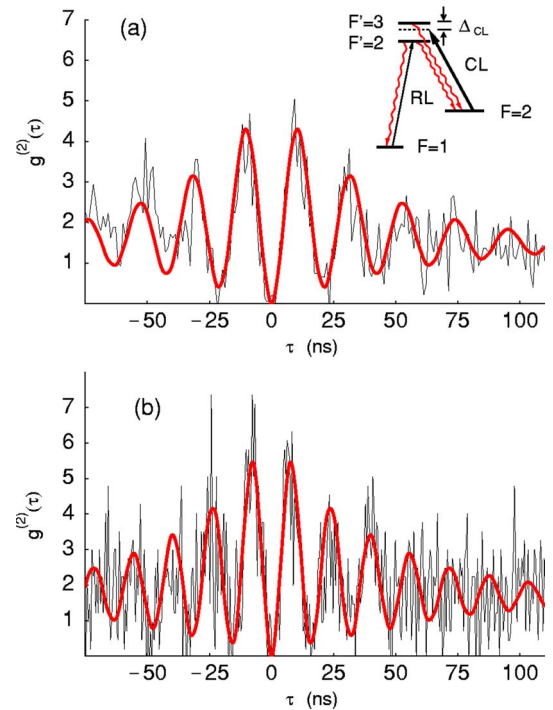

FIG. 4. (Color online) Intensity correlation function $g^{(2)}(\tau)$ (background corrected) of the resonance fluorescence from a single ^{87}Rb atom in the dipole trap for two different trap depths and partial level scheme of ^{87}Rb (inset). Bold line: numerical calculation. Thin line: measured correlation function. Experimental parameters: I_{CL} =103 mW/cm^2, I_{RL}=12 mW/cm^2, $\Delta_{CL}/2\pi=-31$ MHz, dipole trap depth (a) U=0.38 mK, (b) U=0.81 mK.

shows an exponential decay from the asymptotic value 1.24 around $\tau=0$ to 1.0 for large τ with a time constant of 1.8 μs. This effect can be explained by the diffusive atomic motion in the intensity-modulated light field of our three-dimensional cooling beam configuration and was already studied in detail by Gomer *et al.* [28] with a single atom in a MOT.

On short time scales, most prominently we observe an uncorrected minimum value $g^{(2)}(0)=0.52\pm0.14$ at zero delay ($\tau=0$). Taking into account accidental coincidences due to the dark count rate of 300 s^{-1} of each detector, we derive a corrected minimum value $g^{(2)}_{corr}(0)=0.02\pm0.14$. Within our experimental errors this is compatible with perfect photon antibunching of the emitted fluorescence light and therefore proves the single atom character of our dipole trap. Furthermore, we observe the signature of Rabi oscillations due to the coherent interaction of the cooling and repump laser field with the atomic hyperfine levels involved in the excitation process. The oscillation frequency is in good agreement with a simple two-level model [22] and the amplitude is damped out on the expected time scale of the 5 $^2P_{3/2}$ excited state lifetime (=27 ns).

The correlation function of a driven two-level atom shows its maximum value $g^{(2)}_{max}=2$ for τ close to zero [22]. In contrast, the background corrected correlations in Fig. 4 show larger oscillation amplitudes up to a maximum value of 5. This increase of the oscillation amplitude—already known

from experiments with single ions [29,30]—is a consequence of optical pumping among the two hyperfine ground levels $F=1$ and $F=2$. To understand the consequences of this effect on the second-order correlation function in detail one has to take into account the atomic level structure involved in the excitation process.

Four-level model: For the fluorescence detection of a single atom in our dipole trap we use the MOT cooling laser (CL), red detuned to the unperturbed hyperfine transition $5\,^2S_{1/2}$, $F=2 \rightarrow 5\,^2P_{3/2}$, $F'=3$ (inset of Fig. 4) by $\Delta_{CL} = -5\Gamma$ ($\Gamma=2\pi \times 6$ MHz is the natural linewidth). To avoid optical pumping to the $5\,^2S_{1/2}$, $F=1$ hyperfine ground level we additionally shine in a repump laser (RL) on resonance with the unperturbed hyperfine transition $5\,^2S_{1/2}$, $F=1 \rightarrow 5\,^2P_{3/2}$, $F'=2$. Because the atom is stored in a dipole trap the ac Stark effect additionally shifts the cooling and repump light fields out of resonance. This leads to significant atomic population in $F=1$ and therefore to a breakdown of the two-level assumption.

For the following calculation we assume that the repump laser excites the $F'=2$ level, whereas the cooling laser can excite both hyperfine levels $F'=2$ and $F'=3$. These couplings are characterized by the Rabi frequencies Ω_1, Ω_2, and Ω_3, respectively. Because the three pairs of counterpropagating circularly polarized cooling laser beams form an intensity lattice in space and due to the finite kinetic energy of the atom corresponding to a temperature of approximately 105 μK (see next section) it is quite complicated to correctly describe the internal and external dynamics of the atom in the dipole trap potential. In a classical picture the atom oscillates in the trap potential with an amplitude of several optical wavelengths. Hence, during this oscillatory movement the atom experiences both a changing intensity and polarization. This situation suggests simplifying the internal atomic dynamics neglecting the Zeeman substructure of the involved hyperfine levels [see Fig. 4(a), inset] and to treat the exciting cooling and repump light fields as unpolarized with an average intensity of six times the single beam intensity I.

The equation of motion for the atomic density matrix ρ of this system is given by

$$\dot{\rho} = \frac{-i}{\hbar}[H, \rho] + R. \qquad (1)$$

In the rotating-wave approximation (RWA) the matrix representation of the Hamiltonian H—describing the free atom and the interaction with the repump laser field of angular frequency ω_1 and the cooling laser field of angular frequency ω_2—in the basis of the bare atomic states $|a\rangle$, $|b\rangle$, $|c\rangle$, and $|d\rangle$ corresponding to the light-shifted hyperfine levels $F'=2$, $F=1$, $F=2$, and $F'=3$, respectively, is given by

$$H = \frac{-\hbar}{2} \begin{pmatrix} -2\omega_a & \Omega_1 e^{-it\omega_1} & \Omega_2 e^{-it\omega_2} & 0 \\ \Omega_1 e^{it\omega_1} & -2\omega_b & 0 & 0 \\ \Omega_2 e^{it\omega_2} & 0 & -2\omega_c & \Omega_3 e^{it\omega_2} \\ 0 & 0 & \Omega_3 e^{-it\omega_2} & -2\omega_d \end{pmatrix}. \qquad (2)$$

The relaxation term R in the equation of motion (1) represents spontaneous decay [31] from the excited hyperfine

level $F'=3$ to $F=2$ with a decay rate Γ and from $F'=2$ to $F=2$ and $F=1$ with $\Gamma/2$, according to the branching ratio of the respective hyperfine transitions. In a matrix representation we obtain

$$R = \begin{pmatrix} -\Gamma\rho_{aa} & -\dfrac{\Gamma}{2}\rho_{ab} & -\dfrac{\Gamma}{2}\rho_{ac} & -\Gamma\rho_{ad} \\ -\dfrac{\Gamma}{2}\rho_{ba} & \dfrac{\Gamma}{2}\rho_{aa} & 0 & -\dfrac{\Gamma}{2}\rho_{bd} \\ -\dfrac{\Gamma}{2}\rho_{ca} & 0 & \dfrac{\Gamma}{2}\rho_{aa}+\Gamma\rho_{dd} & -\dfrac{\Gamma}{2}\rho_{cd} \\ -\Gamma\rho_{da} & -\dfrac{\Gamma}{2}\rho_{db} & -\dfrac{\Gamma}{2}\rho_{dc} & -\Gamma\rho_{dd} \end{pmatrix}, \qquad (3)$$

where energy relaxation from the $F=2$ to $F=1$ hyperfine ground level is neglected.

The light field, scattered by the atom is described by the electric field operators $\mathbf{E}^+$ and $\mathbf{E}^-$, and the two-photon correlation function $g^2(\tau)$ is given, according to Glauber [32], by

$$g^{(2)}(\tau) = \frac{\langle \mathbf{E}^-(t)\mathbf{E}^-(t+\tau)\mathbf{E}^+(t+\tau)\mathbf{E}^+(t)\rangle}{\langle \mathbf{E}^-(t)\mathbf{E}^+(t)\rangle^2}. \qquad (4)$$

For almost monochromatic light fields and a small detection probability, this function describes the conditional probability of detecting a photon at time $t+\tau$, given the previous detection of another photon at time t, normalized by the probability to detect statistically independent photons. From the numerical solutions of the equation of motion (1) for the atomic density matrix ρ we calculate $g^2(\tau)$ with the help of the quantum regression theorem [33] which relates the two-time expectation values in (4) to particular one-time expectation values and the initial conditions for the density matrix [34]. As we do not distinguish from which hyperfine transition the first photon of a pair-event came from, the initial condition $\rho(t=0)$ for the numerical solution of (1) was calculated from the steady-state solution $\rho(t=\infty)$. The resulting correlation function is then given by the ratio of the excited state populations at time τ and in the steady state ($\tau=\infty$),

$$g^{(2)}(\tau) = \frac{\rho_{aa}(\tau) + \rho_{dd}(\tau)}{\rho_{aa}(\infty) + \rho_{dd}(\infty)}. \qquad (5)$$

For our experimental parameters we calculated the second-order correlation in (5) following the described procedure. To include also the diffusive motion of the atom in the intensity modulated light field of our cooling beam configuration, the resulting correlation function is multiplied with $1+Ae^{-k\tau}$ [28], whereby the parameters A and k have been determined from a fit to the measured correlation function on the μs time scale.

Figure 4 shows the measured, background corrected correlation functions for two different dipole trap depths. Increasing the dipole trap depth U from 0.38 to 0.81 mK without changing the laser cooling parameters enhances the effective detuning of the cooling laser to the hyperfine transition $5\,^2S_{1/2}$, $F=2 \rightarrow 5\,^2P_{3/2}$, $F'=3$ due to an increase of the ac Stark shift of the respective atomic levels in the far-off resonant dipole trap laser field. This effect gives rise to an

increase of the effective Rabi frequency from 47.5 MHz to 62.5 MHz and is directly observed in the respective photon correlation function in Fig. 4.

To summarize, within our experimental errors we find good agreement of the calculated second-order correlation function with the measured correlations. In contrast to a simple two-level model a four-level model is required to correctly describe the observed oscillation amplitude of the $g^{(2)}(\tau)$ function.

IV. SPECTRAL PROPERTIES

In the present experiment a single optically trapped atom is cooled by three-dimensional polarization gradients in an optical molasses. This leads to a final kinetic energy on the order of 100 μK [35]. Due to the motion of the atom in the confining potential the Doppler effect causes a line broadening in the emitted fluorescence spectrum. Hence, a spectral analysis of the emitted resonance fluorescence yields information about the kinetic energy of the trapped atom.

For low excitation intensities the fluorescence spectrum of a two-level atom exhibits an elastic peak centered at the incident laser frequency ω_L, while for higher intensities an inelastic component becomes dominant, with contributions at the frequencies ω_L and $\omega_L \pm \Omega_0$ [36], where Ω_0 denotes the effective Rabi frequency. This so-called "Mollow triplet" arises from the dynamical Stark splitting of the two-level transition and has been observed in a number of experiments, using low-density atomic beams [37–39] or a single trapped and laser-cooled Ba$^+$ ion [40]. Surprisingly, there are only few experimental investigations of the elastic scattering process with a frequency distribution equal to the exciting laser. Subnatural linewidths were demonstrated with atomic beam experiments [39,41], atomic clouds in optical molasses [42,43] and a single trapped and laser-cooled Mg$^+$ ion [44,45].

For our laser cooling parameters the fluorescence spectrum is dominated by elastic Rayleigh scattering [34,36]. Hence, the emitted fluorescence light exhibits the frequency distribution of the exciting laser field (0.6 MHz FWHM) broadened by the Doppler effect. Position-dependent atomic transition frequencies in the dipole trap due to the inhomogeneous ac Stark shift (caused by the finite kinetic energy) give no additional broadening, because the spectrum of the elastically scattered fluorescence light is determined only by the frequency distribution of the exciting light field and not by the atomic transition frequencies.

The scattered fluorescence spectrum is analyzed with a scanning Fabry-Perot interferometer (FPI) with a frequency resolution of 0.45 MHz (FWHM), a transmission of 40%, and a finesse of 370. To measure the spectrum only at times we trap a single atom, a part of the fluorescence light is monitored separately with a reference APD (D1 in Fig. 5). As the broadening of the atomic emission spectrum due to the Doppler effect is small, the instrumental function of the spectrometer and the exciting laser linewidth have to be known accurately. In order to achieve this, we shine a fraction of the exciting light (reference beam) into the collection optics (see Fig. 5). This way, both reference and scattered
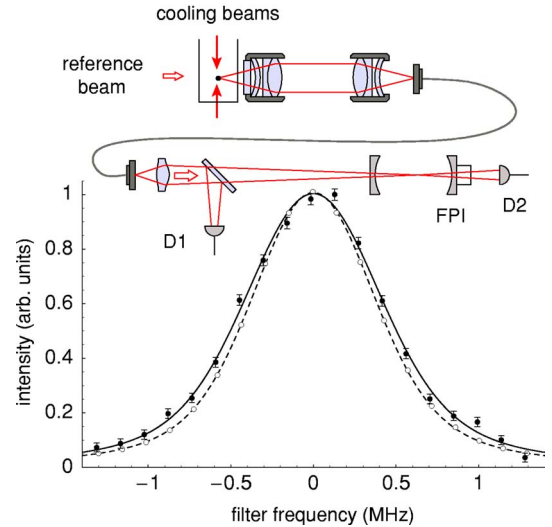

FIG. 5. (Color online) Setup for the measurement of the resonance fluorescence spectrum of light scattered by a single ^{87}Rb atom. Both the atomic fluorescence and the laser light are analyzed alternately with the same scanning FPI. The spectra exhibit a width of 0.90 ± 0.02 MHz and 1.00 ± 0.02 MHz (FWHM) for the excitation (-○-) and the fluorescence light (-●-), respectively. Experimental parameters: $I_{CL} = 87$ mW/cm^2, $I_{RL} = 12$ mW/cm^2, $\Delta_{CL}/2\pi = -19$ MHz, dipole trap depth $U = (0.62 \pm 0.06)$ mK.

light are subject to the identical spectrometer instrumental function, whereby the reference laser spectrum is also used to monitor length drifts of the analyzing cavity. In the experiment, the spectrum of the reference beam and the fluorescence light scattered by the atom were recorded alternately. After each measurement a compensation of the cavity length drift was performed by referencing the cavity frequency to the point of maximum transmission of the reference laser.

With this procedure we obtained the two (normalized) data sets in Fig. 5. As expected, the resonance fluorescence spectrum exhibits a "subnatural" linewidth of 1.00 ± 0.02 MHz (FWHM) because the elastic Rayleigh contribution dominates the scattering process. The exciting laser light field exhibits a linewidth of 0.90 ± 0.02 MHz (FWHM) which is the convolution of the transmission function of the Fabry-Perot resonator with the spectral width of the excitation laser. The depicted error bars reflect the statistical error from the individual count rates of each data point. For the reference laser spectrum this error is too small to be visible in this graph.

For an atom at rest the resonance fluorescence spectrum shows the same linewidth as the exciting light field. Any finite kinetic energy distribution of the atom will lead to a broadening of the atomic emission spectrum and therefore can be used for the determination of the atomic "temperature." To extract the mean kinetic energy from the measured spectra in Fig. 5, we assume that the atom is subject to the same stationary Gaussian velocity distribution in all directions. This assumption is justified because the atom is expected to occupy on average up to 100 motional modes of the dipole trap potential [35]. Therefore the atomic motion can be considered classical and the energy distribution is given by the Boltzmann statistics, leading to a thermal velocity distribution.

According to this assumption we convolve a Gaussian velocity distribution with the measured reference laser line profile. The resulting function is fitted to the data points of the fluorescence spectrum with the variance of the Gaussian profile being the only free fit parameter [47]. From the fitted variance we directly obtain the mean kinetic energy E_{kin} of a single atom in the dipole trap

$$E_{kin} = \frac{1}{2} m \langle \Delta v^2 \rangle = (105 \pm 24)^{+14}_{-17} \ \mu K \times k_B, \qquad (6)$$

with a statistical error of $\pm 24 \ \mu K$. Here k_B denotes the Boltzmann constant, m is the atomic mass, and $\langle \Delta v^2 \rangle$ is the mean quadratic velocity.

The calculation of the mean kinetic energy contains a systematic error because the cooling beams have different angles relative to the axis defined by the dipole trap and the detection optics. The overall Doppler broadening of the elastically scattered fluorescence light depends on these angles. Because the relative intensity of these beams is not known exactly, a systematic error occurs. In order to estimate an upper bound for this error we assume that the atom scatters light only from the beams which would give the highest or lowest velocities, respectively. From this estimation we obtain the last two error bounds in (6). Within the experimental errors, the measured temperature is equal to or smaller than the Doppler temperature of ^{87}Rb (146 μK).

V. SUMMARY

We have studied the nonclassical properties of fluorescence light scattered by a single optically trapped ^{87}Rb atom. For this purpose, we have set up a HBT experiment and measured the second-order correlation function of the detected fluorescence light. The measured two-photon correlation function exhibits strong photon antibunching verifying the presence of a single trapped atom. Due to inelastic two-body collisions which are present during the loading stage of the dipole trap and the small trap volume [11], only a single atom per time was trapped. Furthermore, the measured second-order correlation function shows the internal and external dynamics of the atomic hyperfine levels involved in the excitation process. An atomic four-level model was developed and its predictions were compared with the measured second-order correlation functions. Within the experimental errors we find good agreement of the calculated predictions with the measured data.

In addition, the spectrum of the emitted resonance fluorescence was measured. We find that the atom-light interaction is dominated by elastic Rayleigh scattering. Due to the Doppler effect, we observed an additional broadening of the atomic fluorescence spectrum. From this we determined the mean kinetic energy of the trapped atom corresponding to a temperature of 105 μK.

This simple single-atom trap is a promising tool for the effective generation of narrow-band single photons [46] and for the realization of a quantum memory for light [4]. Furthermore, our setup can also be used for the generation of entanglement between the spin state of a single ^{87}Rb atom and the polarization state of a spontaneously emitted single photon [5]. This kind of atom-photon entanglement will close the link between atoms and photons in quantum information applications and opens the possibility to entangle atoms at large distances, well suited for a loophole-free test of Bell's inequality [1,2,5].

[1] K. Saucke, Diploma thesis, Ludwig-Maximilians-Universität, München (2002).

[2] C. Simon and W. T. M. Irvine, Phys. Rev. Lett. **91**, 110405 (2003); L.-M. Duan and H. J. Kimble, *ibid.* **90**, 253601 (2003); X. L. Feng, Z. M. Zhang, X. D. Li, S. Q. Gong, and Z. Z. Xu, *ibid.* **90**, 217902 (2003).

[3] B. B. Blinov, D. L. Moehring, L.-M. Duan, and C. Monroe, Nature (London) **428**, 153 (2004).

[4] D. N. Matsukevich and A. Kuzmich, Science **306**, 663 (2004); B. Julsgaard, J. Sherson, J. I. Cirac, J. A. Fiurasek, and E. S. Polzik, Nature (London) **432**, 482 (2004).

[5] J. Volz, M. Weber, D. Schlenk, W. Rosenfeld, J. Vrana, K. Saucke, C. Kurtsiefer, and H. Weinfurter, Phys. Rev. Lett. **96**, 030404 (2006).

[6] M. A. Nielsen and I. L. Chuang, *Quantum Computation and Quantum Information* (Cambridge University Press, Cambridge, 2000).

[7] H.-J. Briegel, W. Dür, J. I. Cirac, and P. Zoller, Phys. Rev. Lett. **81**, 5932 (1998).

[8] W. Neuhauser, M. Hohenstatt, P. E. Toschek, and H. Dehmelt, Phys. Rev. A **22**, 1137 (1980).

[9] F. Diedrich and H. Walther, Phys. Rev. Lett. **58**, 203 (1987).

[10] A. Kuhn, M. Hennrich, and G. Rempe, Phys. Rev. Lett. **89**, 067901 (2002).

[11] N. Schlosser, G. Reymond, I. Protsenko, and P. Grangier, Nature (London) **411**, 1024 (2001).

[12] C. Brunel, B. Lounis, P. Tamarat, and M. Orrit, Phys. Rev. Lett. **83**, 2722 (1999).

[13] B. Lounis and W. E. Moerner, Nature (London) **407**, 491 (2000).

[14] C. Kurtsiefer, S. Mayer, P. Zarda, and H. Weinfurter, Phys. Rev. Lett. **85**, 290 (2000).

[15] R. Brouri, A. Beveratos, J.-P. Poizat, and P. Grangier, Opt. Lett. **25**, 1294 (2000).

[16] P. Michler *et al.*, Science **290**, 2282 (2000).

[17] C. Santori, M. Pelton, G. Solomon, Y. Dale, and Y. Yamamoto, Phys. Rev. Lett. **86**, 1502 (2001).

[18] J. D. Miller, R. A. Cline, and D. J. Heinzen, Phys. Rev. A **47**, R4567 (1993).

[19] R. A. Cline, J. D. Miller, M. R. Matthews, and D. J. Heinzen, Opt. Lett. **19**, 207 (1994); D. Frese *et al.*, Phys. Rev. Lett. **85**, 3777 (2000).

[20] D. DiVicenzo, Fortschr. Phys. **48**, 771 (2000).

[21] N. Schlosser, G. Reymond, and P. Grangier, Phys. Rev. Lett.

89, 023005 (2002).

[22] H. J. Carmichael and D. F. Walls, J. Phys. B **9**, 1199 (1976).

[23] R. Grimm, M. Weidemüller, and Y. B. Ovchinnikov, e-print physics/9902072.

[24] C. Monroe, W. Swann, H. Robinson, and C. Wieman, Phys. Rev. Lett. **65**, 1571 (1990).

[25] S. J. M. Kuppens, K. L. Corwin, K. W. Miller, T. E. Chupp, and C. E. Wieman, Phys. Rev. A **62**, 013406 (2000).

[26] J. C. Bergquist, R. G. Hulet, W. M. Itano, and D. J. Wineland, Phys. Rev. Lett. **57**, 1699 (1986); W. Nagourney, J. Sandberg, and H. Dehmelt, *ibid.* **56**, 2797 (1986); T. Sauter, W. Neuhauser, R. Blatt, and P. E. Toschek, *ibid.* **57**, 1696 (1986).

[27] S. Reynaud, Ann. Phys. (Paris) **8**, 351 (1983).

[28] V. Gomer *et al.*, Appl. Phys. B: Lasers Opt. **B67**, 689 (1998).

[29] M. Schubert, I. Siemers, R. Blatt, W. Neuhauser, and P. E. Toschek, Phys. Rev. Lett. **68**, 3016 (1992).

[30] M. Schubert, I. Siemers, R. Blatt, W. Neuhauser, and P. E. Toschek, Phys. Rev. A **52**, 2994 (1995).

[31] R. K. Wangsness and F. Bloch, Phys. Rev. **89**, 728 (1953).

[32] R. J. Glauber, Phys. Rev. **130**, 2529 (1963); **131**, 2766 (1963).

[33] M. Lax, Phys. Rev. **145**, 110 (1966).

[34] C. Cohen-Tannoudji, J. Dupont-Roc, and G. Grynberg, *Atom-Photon Interactions* (Wiley, New York, 1998).

[35] B. M. Garraway and V. G. Minogin, Phys. Rev. A **62**, 043406 (2000).

[36] B. R. Mollow, Phys. Rev. **188**, 1969 (1969).

[37] F. Schuda, C. R. Stroud, and M. Hercher, J. Phys. B **1**, L198 (1974).

[38] F. Y. Wu, R. E. Grove, and S. Ezekiel, Phys. Rev. Lett. **35**, 1426 (1975).

[39] W. Hartig, W. Rasmussen, R. Schieder, and H. Walther, Z. Phys. A **278**, 205 (1976).

[40] Y. Stalgies, I. Siemers, B. Appasamy, T. Altevogt, and P. E. Toschek, Europhys. Lett. **35**, 259 (1996).

[41] H. M. Gibbs and T. N. C. Venkatesan, Opt. Commun. **17**, 87 (1976).

[42] C. I. Westbrook *et al.*, Phys. Rev. Lett. **65**, 33 (1990).

[43] P. S. Jessen *et al.*, Phys. Rev. Lett. **69**, 49 (1992).

[44] J. T. Höffges, H. W. Baldauf, W. Lange, and H. Walther, J. Mod. Opt. **44**, 1999 (1997).

[45] J. T. Höffges, H. W. Baldauf, T. Eichler, S. R. Helmfrid, and H. Walther, Opt. Commun. **133**, 170 (1997).

[46] B. Darquié *et al.*, Science **309**, 454 (2005).

[47] This procedure is justified because the statistical error on the data points of the reference laser spectrum is much smaller than the error on the fluorescence data.